research article

Determination of dosimetric parameters for shielded ^{153}Gd source in prostate cancer brachytherapy

Mahdi Ghorbani[1], Benyamin Khajetash[2], Najmeh Ghatei[3], Mohammad Mehrpouyan[4], Ali S. Meigooni[5], Ramin Shahraini[4]

[1] Biomedical Engineering and Medical Physics Department, Faculty of Medicine, Shahid Beheshti University of Medical Sciences, Tehran, Iran
[2] Medical Physics Department, School of Medicine, Iran University of Medical Sciences, Tehran, Iran
[3] Radiotherapy Department, Namazi Hospital, Shiraz, Iran
[4] Radiology and Radiotherapy Department, Faculty of Medicine, Sabzevar University of Medical Sciences, Sabzevar, Iran
[5] Comprehensive Cancer Centers of Nevada, Las Vegas, Nevada, USA

Radiol Oncol 2017; 51(1): 101-112.

Received 22 June 2016
Accepted 27 December 2016

Correspondence to: Behyamin Khajetash, Medical Physics Department, School of Medicine, Iran University of Medical Sciences, Hemmat Highway, Tehran, Iran.E-mail: benyamin.khajetash@gmail.com and Mohammad Mehrpouyan, Radiology and Radiotherapy Department, Faculty of Medicine, Sabzevar University of Medical Sciences, Sabzevar, Iran. E-mail: mehrpouyan.mohammad@gmail.com

Disclosure: No potential conflicts of interest were disclosed.

Both Corresponding authors have equal benefits

Background. Interstitial rotating shield brachytherapy (I-RSBT) is a recently developed method for treatment of prostate cancer. In the present study TG-43 dosimetric parameters of a ^{153}Gd source were obtained for use in I-RSBT.

Materials and methods. A ^{153}Gd source located inside a needle including a Pt shield and an aluminum window was simulated using MCNPX Monte Carlo code. Dosimetric parameters of this source model, including air kerma strength, dose rate constant, radial dose function and 2D anisotropy function, with and without the shields were calculated according to the TG-43 report.

Results. The air kerma strength was found to be 6.71 U for the non-shielded source with 1 GBq activity. This value was found to be 0.04 U and 6.19 U for the Pt shield and Al window cases, respectively. Dose rate constant for the non-shielded source was found to be 1.20 cGy/(hU). However, for a shielded source with Pt and aluminum window, dose rate constants were found to be 0.07 cGy/(hU) and 0.96 cGy/(hU), on the shielded and window sides, respectively. The values of radial dose function and anisotropy function were tabulated for these sources. Additionally, isodose curves were drawn for sources with and without shield, in order to evaluate the effect of shield on dose distribution.

Conclusions. Existence of the Pt shield may greatly reduce the dose to organs at risk and normal tissues which are located toward the shielded side. The calculated air kerma strength, dose rate constant, radial dose function and 2D anisotropy function data for the ^{153}Gd source for the non-shielded and the shielded sources can be used in the treatment planning system (TPS).

Key words: interstitial rotating shield brachytherapy; ^{153}Gd; TG-43 dosimetric parameters; Monte Carlo simulation

Introduction

Prostate cancer is the most common cancer in men. In 2013, it was reported that the number of 2,850,139 men were living with prostate cancer in the United States.[1] The number of new cases of prostate cancer from the year 2009 to 2013, was 129.4 per 100,000 men per year and the number of deaths caused by prostate cancer was 20.7 per 100,000 men per year.[1] This cancer is observed with a higher prevalence in African-American men than in white men.[2] Brachytherapy is one of the com-

mon therapeutic methods for treatment of prostate cancer. This approach has shown successful outcomes in treatment of this cancer. The success of brachytherapy is due to advantages such as simple performance and reduced side effects of treatment compared to external radiation therapy and surgical removal of the tumor.[3-6] Brachytherapy is a treatment in which one or a number of covered radioactive sources are inserted at a short distance from the target. Brachytherapy is performed either as intracavitary procedure, in which the brachytherapy source is placed inside the natural body cavity, adjacent to the tumor. The second method is interstitial brachytherapy, in which brachytherapy seeds are implanted directly inside the tumor mass. With this treatment method, the required amounts of radiation dose can be delivered to the tumor with the rapid dose fall off to the healthy tissues around the tumor.

Originally, brachytherapy treatments were performed with ^{226}Ra sources. Nowadays, the use of artificial radionuclides such as ^{125}I, ^{131}Cs, and ^{103}Pd is rapidly increasing.[7-9] Presently, brachytherapy sources are widely used for treatment of various types of cancer patients. ^{153}Gd is a medium energy brachytherapy source emitting photons in the range of 40 to 100 keV. This isotope has a low dose rate and its half-life is 242 days. Interstitial rotating shield brachytherapy (I-RSBT) is a type of brachytherapy in which a shield is used to spare normal tissues from radiation damage. The rotating capability enables the user to select an emission angle to direct the radiation to a specified tumor. It can also be used in sequencing the rotating shield in dynamic rotational shield brachytherapy. With I-RSBT it is possible to have a significant dose reduction in urethra while delivering higher prostate organ dose. The main reason for the use of ^{153}Gd in I-RSBT method is that it requires less shielding within the source than other higher energy isotopes such as iridium.

The main goal of any radiation therapy treatment is to maximize the dose to the tumor while limiting the dose to adjacent normal tissue and organs. Therefore, shielding the sensitive organs around the target volume has always been one of the important issues. In brachytherapy of prostate and cervix, the sensitive organs such as the rectum and bladder should be protected to receive the radiation dose lower than their tolerance level. For the purpose (I-RSBT), the use of special cylindrically shielded source can reach the aim. The shield there is a platinum sleeve with an aluminium gap leaking the narrow source beam. The difficulty of manufacturing of a shielded source is in its limited size. Namely, the cylindrical source should be capable to enter the hollow brachytherapy needle with the diameter *e.g.* 1.6 gauge. Energetic sources (Ir-192) need more shielding thickness which prevents them entering the small diameter brachytherapy needles.

The report by task group No. 43 (TG-43) from American Association of Physicists in Medicine is known as the most common formalism for calculation of the dose distribution around brachytherapy sources. According to this protocol, dosimetric parameters around brachytherapy sources are obtained by experimental measurement or simulation techniques using the Monte Carlo codes in a uniform water phantom.[10-11] Monte Carlo is a computational technique for solving problems in various fields including physical and mathematical sciences. This method is based on random sampling to achieve the required results. Different Monte Carlo codes are currently used in medical radiation physics: MCNP, EGSnrc, GEANT4, SIMIND, etc. Monte Carlo N-Particle (MCNP) is specially designed for nuclear application of radiation transport but it also can be used for other fields, for example in medical physics applications. Monte Carlo codes are of high capabilities in particle transport physics lacking applications in practical medical physics dosimetric problems.[12-14] These methods can have desired results to assess dosimetric parameters such as air kerma strength, dose rate constant, radial dose function and anisotropy function of brachytherapy sources.[15,16] In a number of previous studies, dosimetric parameters of hypothetical brachytherapy sources were calculated prior to their fabrications in order to assess the feasibility of its fabrication. One of these sources is ^{153}Gd that has been introduced by Enger *et al*.[17] Additionally, ^{153}Gd radionuclide has been recently used in nuclear medicine imaging systems *e.g.* linear scanners and quality assurance procedures such as phantom calibrations.

In radiotherapy the radiation dose destroys the tumor cells causing the healing of cancer and improving the patient's quality of life. There is a need in prostate brachytherapy to reduce the dose to radiosensitive organs such as rectum and bladder reducing the dose side effects to these sensitive organs. Therefore, in a proper patient treatment plan the amount of absorbed dose to critical organs should be exactly specified and controlled.[18]

Interstitial rotating shield brachytherapy is a new type of high dose rate brachytherapy in which the radiation dose is delivered by shielded

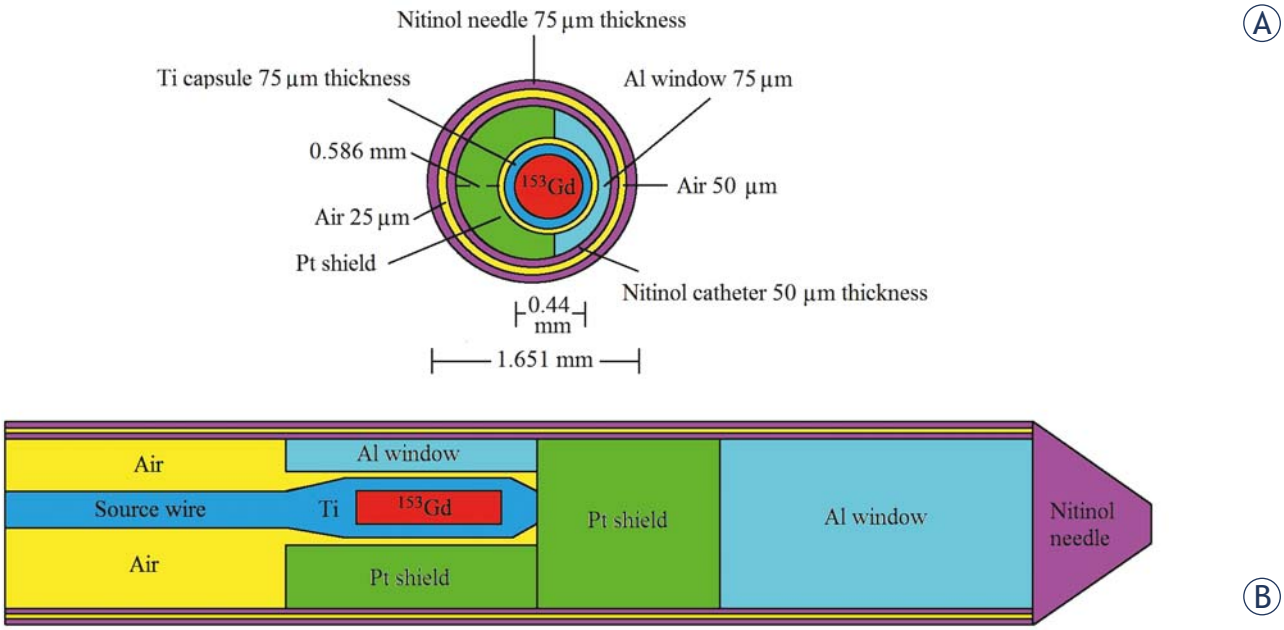

FIGURE 1. A schematic view of the simulated ^{153}Gd source, Nitinol needle including Pt shields and Al windows. **(A)** transverse view, **(B)** longitudinal view. This figure is not in to a real scale. Polar angles that were used to calculate the anisotropy function.

and rotating catheters. In I-RSBT a brachytherapy source has a well-defined shield with the capability of rotation around the source's longitudinal axis to spare normal tissues. With I-RSBT the limitation that dose distributions should be symmetric around a brachytherapy source is resolved. Therefore, with this method there is the potential to deliver unrivalled dose distributions.[19] In a recent study conducted by Adams *et al*.[19], the interstitial rotating shield brachytherapy (I-RSBT) method was introduced for brachytherapy of prostate. In that study the method was presented to reduce the dose to rectum, bladder and urethra in I-RSBT with a ^{153}Gd source. They have demonstrated that brachytherapy with rotational shield has the potential to reduce the dose to organs at risk compared to traditional brachytherapy. The isodose curves around the shielded ^{153}Gd source were compared with the isodose curves of an^{192}Ir source. Additionally, they introduced the data related to an anonymous patient in a treatment planning system and compared dose volume histograms from conventional brachytherapy with ^{192}Ir source with those from ^{153}Gd based I-RSBT. However, in that study TG-43 dosimetric parameters of the source with shield were not investigated. Enger *et al*.[17] introduced a hypothetical ^{153}Gd source and calculated TG-43 parameters for the source without rotational shield. In that study, the hypothetical ^{153}Gd source was introduced for potential use in I-RSBT. However, only TG-43 parameters were determined and the effect of rotational shield geometry on dosimetric aspects was not evaluated. In another study Ghorbani and Behmadi[20] calculated TG-43 parameters for the same hypothetical nonshielded ^{153}Gd source and compared them with dosimetric parameters of commercially available ^{192}Ir and ^{125}I sources. In the study by Ghorbani and Behmadi the effect of shielding was not considered, as it was not evaluated by the study of Enger *et al*.[7] In the aforementioned studies TG-43 parameters of a shielded ^{153}Gd source were not evaluated.

Consequently the present study evaluates a ^{153}Gd source for use in the I-RSBT and its dosimetric parameters are obtained according to TG-43 formulation for use in prostate brachytherapy.

Materials and methods

Geometry of ^{153}Gd source

In our study the design of a ^{153}Gd source, a needle including Pt shields and Al windows were adopted from the study by Adams *et al*.[19] The geometry of the ^{153}Gd source is designed so that the active part of this source is a cylinder with length of 10 mm and diameter of 440 µm. The source has an activity of 62 GBq. Having the activity of the source, it is possible to normalize a dosimetric quantity to that activity. For example by having this ^{153}Gd source

TABLE 1. The energy spectrum of ^{153}Gd radionuclide.[18] In these data, the energy values were rounded to two decimal places

Energy (keV)	Prevalence (%)
5.18	0.374
5.82	0.976
5.82	0.1341
5.85	8.86
6.44	0.559
6.46	5.64
6.57	0.9214
6.62	0.0845
6.84	1.8512
7.48	0.947
7.77	0.173
7.79	0.244
14.06	0.0183
21.20	0.0224
40.47	0.00953
40.90	35.29
41.54	63.516
46.90	6.2516
47.04	12.13
47.37	0.1848
48.25	4.001
48.39	1.597
54.19	40.01622
69.67	2.41923
75.42	0.078323
83.37	0.1964
89.49	0.0694
96.88	0.0022
97.43	29
103.18	21.1123
118.11	0.000121
166.56	0.00033
172.30	0.00022
172.85	0.036017

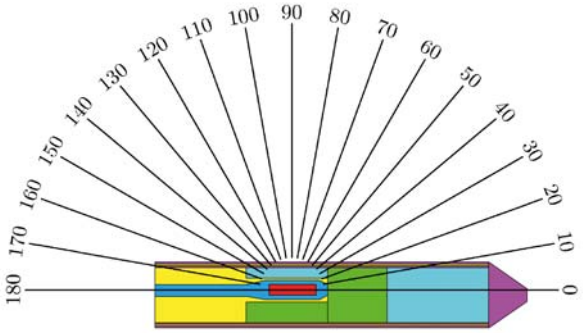

FIGURE 2. Polar distribution of angles in calculation of anisotropy function in the shielded mode.

with 62 GBq activity and by dividing a quantity of this source to 62 GBq it is feasible to calculate that quantity per GBq. The active core is surrounded by 75 μm titanium capsule with a density of 4.506 g/cm^3. At one side of the titanium capsule there is a window of pure aluminum with 2.70 g/cm^3 density and the thickness of 75 μm. On the other side of the source construction, there is a Pt shield which is an alloy of 90% Pt and 10% Ir expressed in weight percentages. The density of this shield is 21.45 g/cm^3. The radioactive source is within Nitnol catheter and a Nitinol needle (Figure 1). These are composed of Ni and Ti with 55.6% and 44.4% percentage weight fractions, respectively. The density of the catheter and needle was considered as 6.54 g/cm^3. The outer diameter of the needle is 1.651 mm. Figure 1 illustrates transverse and longitudinal views of the ^{153}Gd source, catheter, and the needle including the Pt shield and Al windows. It should be noticed that some of the dimensions in this Figure are based on the study by Adams *et al.*[19], while the others are based on assumptions. In other words, we assumed all the dimensions which were not directly reported in the study by Adams *et al.* The photon spectrum of the ^{153}Gd radionuclide is listed in Table 1.[21]

Calculation of dosimetric parameters

According to TG-43U1 report[10], dose distribution around a brachytherapy source can be obtained using the following equation:

$$\dot{D}(r,\theta) = S_K \Lambda \frac{G(r,\ \theta)}{G(r_0,\theta_0)}\ g(r)F(r,\theta) \qquad [1]$$

In this equation the S_K, Λ, $G(r, \theta)$, $g(r)$ and $F(r, \theta)$, are air kerma strength, dose rate constant, geometry function, radial dose function and anisotropy function.

The TG-43U1 quantities agenda are as follows:

MCNPX (version 2.6.0) Monte Carlo simulation code was used to calculate the TG-43 dosimetric parameters of the ^{153}Gd source. The parameters including air kerma strength, dose rate constant, radial dose function and anisotropy function were calculated for the source with the shield and without it.

To calculate the air kerma strength in the non-shielded mode, the source was assumed to be inside a vacuum sphere with a radius of 100 cm. Then, the spherical tally cells were placed at distances ranging from 1 to 40 cm from the source center at 1 cm intervals. These spheres were made of air and their radii were defined according to a joint report from AAPM and European Society for Therapeutic Radiology and Oncology (ESTRO).[22] The amount of air kerma was scored by F6 tally (in terms of MeV/g). Throughout this project the energy cut off for photons and electrons was defined as 1 keV. Each simulation was performed for 1.4×10^9 particles and the maximum type A uncertainty of Monte Carlo simulation in these calculations was 3.08%. The uncertainty quantity in tally calculation is normally listed in the output file of a Monte Carlo program. For the shielded source, the implementation of the program and the calculation of air kerma strength was similar to the non-shielded source. In calculation of air kerma strength for the Pt shield case, the scoring spheres were defined on the Pt shield side. In calculation for the Al window case, the scoring spheres were defined on the Al window side. The maximum type A uncertainties of Monte Carlo simulation calculations in the calculation of air kerma strength for the Pt shield and Al window cases were 32.78% and 3.24%, respectively.

Calculation of dose rate constant was performed based on the formalism presented in the TG-43 report. In the non-shield mode, the ^{153}Gd source was defined in a water sphere with 100 cm radius and a spherical water tally cell with 0.005 cm radius was defined at 1 cm distance from the source. Then, *F4 tally was calculated in combination with mass energy absorption coefficient in order to score the energy deposition per mass. Mass energy absorption coefficients of water listed in Table 4 of National Institute of Standards and Technology (NIST) webpage were used.[23] This program was run for 1.2×10^9 particles and the type A Monte Carlo uncertainty was obtained as 0.34% that is related to statistical fluctuation of the simulation data. By dividing the absorbed dose rate to air kerma strength, the dose rate constant was achieved. In the shielded source

TABLE 2. Radial dose function values for the non-shield and shield modes. The shield mode is related to the Pt and Al window sides

g(r)			
r (cm)	Without shield	With shield	
		Pt shield side	Al window side
0.5	0.90	0.52	0.93
1	1.00	1.00	1.00
1.5	1.06	1.39	1.04
2	1.11	1.73	1.04
2.5	1.13	2.03	1.07
3	1.18	2.22	1.07
3.5	1.14	2.44	1.07
4	1.19	2.72	1.05
5	1.17	2.65	1.02
8	1.01	3.01	0.91
10	0.89	2.63	0.80
12	0.77	2.44	0.71

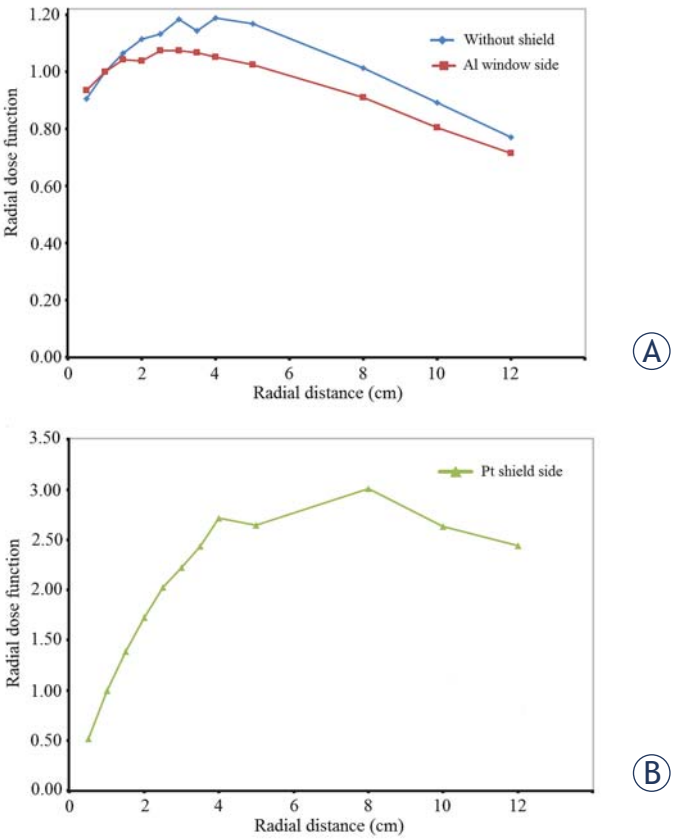

FIGURE 3. (A) Radial dose function for the ^{153}Gd source without the shield and with the shield on Al window side **(B)** radial dose function for the shielded source at Pt shield side.

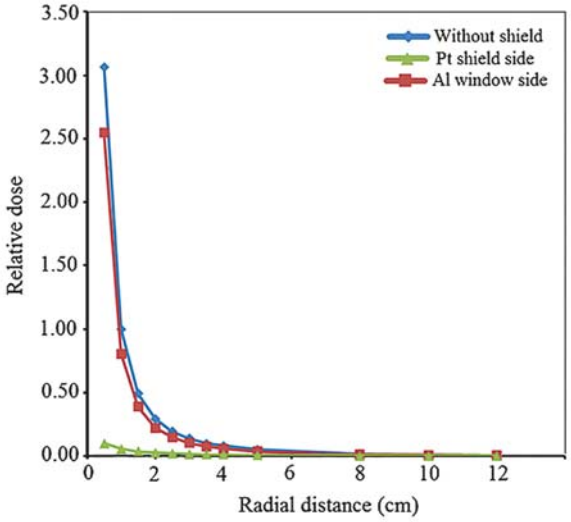

FIGURE 4. Relative dose in non-shielded mode, Pt shield side and aluminum window side in the shielded mode of the source. The normalization point is at 1 cm for the non-shielded case.

cases the calculations were performed for both sides of source. In the calculation of dose rate constant in each case, the dose rate at 1 cm was divided by the air kerma strength for the non-shielded case. The type A uncertainties in Monte Carlo simulations were 0.37% and 1.50% for the calculation at Al window and Pt shield sides, respectively. The other details of the simulations for the shielded source were the same as the simulation details for the non-shielded source.

Radial dose function for the non-shielded source was calculated by selecting a spherical water phantom with 100 cm radius and placing spherical water tally cells at distances ranging from 0.5 cm to 12 cm with 0.5 cm intervals, relative to the source center. The radii of these tally cells were defined according to the report by AAPM and ESTRO[22], in other words, for distances less than 1 cm the radius of the spheres was considered as 0.005 cm, and for distances 1 cm ≤ r<5 cm the radius was considered as 0.025 cm and for distances 5 cm ≤ r< 10 cm the radius was considered 0.05 cm and finally for distances more than 10 cm the radius was considered to be 0.1 cm. In this program *F4 tally was scored and the tally outputs in various energy bins were multiplied by mass energy absorption coefficients using DE and DF cards in MCNP code. Based on the MCNP manual, "DE" and "DF" stand for dose energy and dose function, respectively. In DE cards, energy bins are defined, while in DF card mass energy absorption coefficients are introduced. The program was run for 1.2 × 10^9 particles and the maximum type A Monte Carlo uncertainty was 1.81%. A similar program was defined for the shielded case so that the source was defined in a water sphere with 100 cm radius and also the same intervals and water spheres were defined. Unlike the previous case in this program, spheres were defined on both sides of the source. In this program the output data were obtained using *F4 tally and "DE" and "DF" cards. This program was run for 1.2 × 10^9 particles. The maximum Monte Carlo uncertainty in these investigations in the non-shielded case was observed as 2.07% and in the case of the Pt shield it was observed as 4.49%. It can be considered that the values of these uncertainties are different at different parts of the simulation, and it is because the uncertainty depends on the complexity of geometry, tally type used, number of particle histories, etc.

To calculate the anisotropy function in the case of non-shielded source, a water sphere with 100 cm radius was defined as the phantom. In order to obtain anisotropy function, spheres were defined at different radial distances and angles. These spheres were defined at distances of 0.5, 1, 2, 3, 5, 10 and 12 cm. The angles were ranging from 0 to 180 degrees with 10 degrees intervals. The energy flux was scored in these spheres using *F4 tally. In the calculation of this program mass energy absorption coefficient was utilized. The radius of each sphere was considered according to the report by AAPM and ESTRO. This program had been run for 2 × 10^9 photons and the maximum uncertainty in the Monte Carlo calculation was observed as 1%. The calculations defined for the shielded source were performed similar to the non-shielded source. The difference was that the spheres were on both sides (Pt shield side and Al window side). The uncertainty in the calculation in this case was observed less than 5%. Polar angles that were used to calculate the anisotropy function of the Pt shield case are illustrated in Figure 2. Based on this Figure zero angle begins from the tip of the source for the Pt shield case. For the rest of the cases (nonshielded source and the Al window case) the polar angles are likewise.

Results

Air kerma strength per source activity (per GBq) for the non-shielded mode was obtained equal to 6.71 $cGyh^{-1}cm^2GBq^{-1}$. Based on this value for the nonshielded ^{153}Gd source, 1 U is equal to 4.03 mCi. This value was found to be 0.04 $cGyh^{-1}cm^2GBq^{-1}$

TABLE 3. Anisotropy function values for the ^{153}Gd source at different distances for the non-shielded mode

θ (degrees)	r (cm)					
	0.5	1	2	3	5	10
0	0.71	0.59	0.48	0.41	0.29	-
10	0.75	0.63	0.58	0.51	0.44	0.75
20	0.82	0.76	0.69	0.64	0.63	0.81
30	0.86	0.83	0.77	0.75	0.76	0.86
40	0.90	0.85	0.85	0.84	0.87	0.91
50	0.95	0.91	0.90	0.90	0.93	0.94
60	0.95	0.98	0.94	0.94	0.96	0.96
70	1.00	0.96	0.97	0.98	0.98	0.97
80	0.99	0.99	0.97	0.98	1.01	1.00
90	1.00	1.00	1.00	1.00	1.00	1.00
100	0.97	0.97	0.99	1.00	1.01	1.00
110	1.01	0.95	0.97	0.97	0.96	0.97
120	0.97	0.95	0.92	0.94	0.96	0.97
130	0.95	0.93	0.89	0.90	0.93	0.94
140	0.92	0.87	0.85	0.84	0.87	0.90
150	0.88	0.80	0.78	0.76	0.79	0.87
160	0.83	0.74	0.68	0.65	0.63	0.81
170	0.76	0.65	0.56	0.50	0.45	0.75
180	0.69	-	-	-	-	-

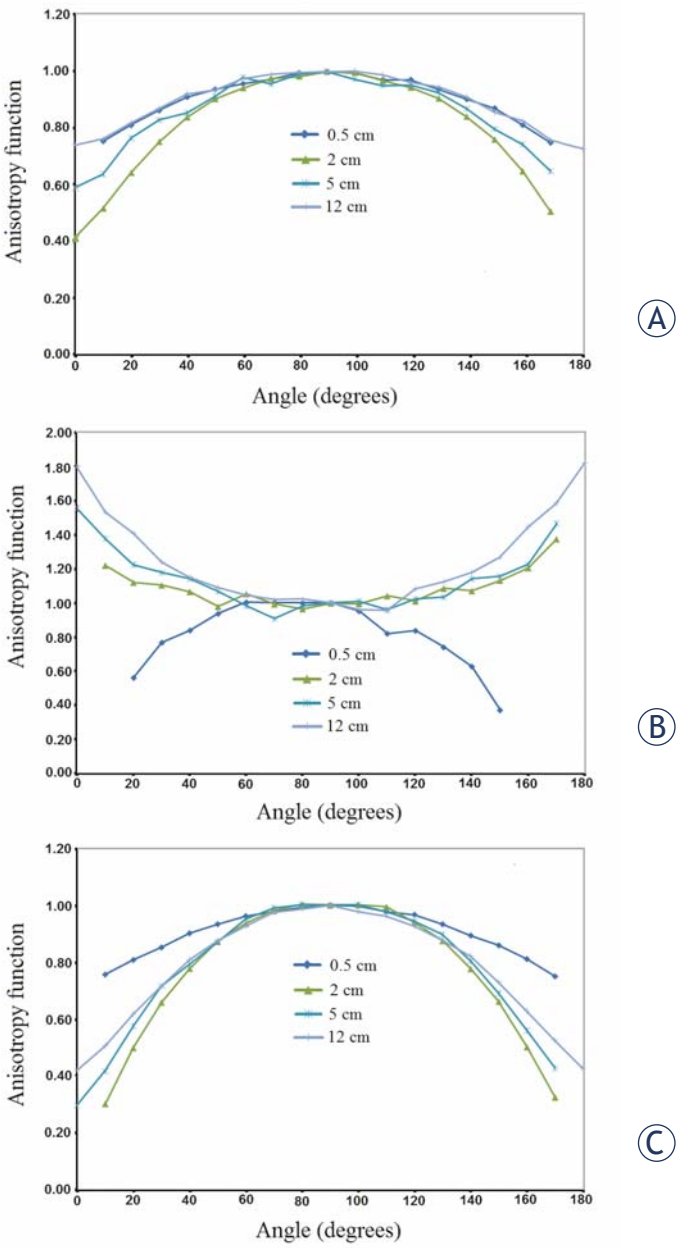

FIGURE 5. Anisotropy function for the ^{153}Gd source: **(A)** non-shielded mode, **(B)** shielded mode, Pt shield side, **(C)** shielded mode, Al window side.

and 6.19 cGyh^{-1}cm^{2}GBq^{-1} for the Pt shield and Al window cases, respectively. The values of dose rate constant for the non-shielded mode was obtained as 1.20 cGyh^{-1}U^{-1} and for the shielded mode for the Pt shield and Al window sides were achieved as 0.07 cGyh^{-1}U^{-1} and 0.96 cGyh^{-1}U^{-1}, respectively. It should be noted that in calculation of dose rate constant for these three cases the dose rate at the reference point (at 1 cm and 90 degrees angle) in each case was divided by the air kerma strength value for the non-shielded source. It can be noted that in the shielded case the dose rate constant is reduced.

Radial dose function values for ^{153}Gd source are listed in Table 2. The first column there refers to the source without shield, the second column refers to the Pt shield side of the source and the third column refers to the Al window side of the source. The radial dose function values are plotted in the Figure 3B for the Pt shield side. Figure 4 shows the relative dose for the non-shielded mode of the source, the Pt shield and Al window sides of the shielded source. In this graph, for all three cases, the dose values have been normalized to the dose at 1 cm distance of the non-shielded source.

Anisotropy function values for the ^{153}Gd source were calculated for 0.5, 1, 2, 3, 5, 10 and 12 cm distances from the source at 19 different angles (ranging from 0 to 180 degrees) with angular intervals of 10 degrees. The results of anisotropy function are presented in Table 3 and Table 4 for the non-shielded and shielded cases, respectively. Figure 5A also shows anisotropy function values at different distances from the source for non-shielded mode. In

TABLE 4. Anisotropy function values for the ^{153}Gd source at different distances for the shielded mode at the Pt and Al windows sides

θ (degree)	r (cm)													
	Pt shield side							Al window side						
	0.5	1	2	3	5	10	12	0.5	1	2	3	5	10	12
0	0.42	0.39	0.30	-	-	-	-	1.80	1.78	1.56	-	-	-	-
10	0.51	0.52	0.42	0.35	0.31	0.29	0.76	1.54	1.57	1.38	1.32	1.22	0.35	-
20	0.62	0.61	0.58	0.51	0.50	0.55	0.81	1.41	1.36	1.23	1.21	1.12	0.88	0.38
30	0.72	0.71	0.72	0.66	0.66	0.70	0.85	1.24	1.31	1.18	1.17	1.10	0.87	0.56
40	0.81	0.81	0.79	0.77	0.78	0.81	0.90	1.15	1.23	1.14	1.07	1.07	1.05	0.77
50	0.88	0.88	0.87	0.86	0.87	0.90	0.93	1.09	1.14	1.07	1.08	0.98	0.86	0.84
60	0.93	0.91	0.95	0.92	0.94	0.97	0.96	1.05	1.07	0.98	1.06	1.05	0.91	0.94
70	0.98	0.96	0.99	0.97	0.98	1.01	0.98	1.02	1.07	0.91	1.04	0.99	1.03	1.00
80	0.99	0.99	1.00	1.00	1.00	1.06	0.99	1.02	1.01	0.98	0.99	0.96	1.00	1.00
90	1.00	1.00	1.00	1.00	1.00	1.00	1.00	1.00	1.00	1.00	1.00	1.00	1.00	1.00
100	0.98	0.99	1.00	0.98	1.00	1.02	1.00	0.96	1.01	1.01	1.04	0.99	1.03	1.00
110	0.96	0.97	0.98	0.97	0.99	0.97	0.98	0.96	1.07	0.96	1.01	1.04	0.99	0.95
120	0.93	0.93	0.95	0.92	0.94	0.96	0.97	1.08	1.09	1.02	1.07	1.01	1.08	0.82
130	0.88	0.89	0.90	0.88	0.88	0.93	0.93	1.13	1.24	1.03	1.07	1.09	0.95	0.84
140	0.82	0.83	0.81	0.77	0.78	0.84	0.89	1.18	1.21	1.14	1.12	1.07	1.04	0.74
150	0.73	0.70	0.69	0.67	0.66	0.71	0.86	1.27	1.29	1.16	1.15	1.13	0.87	0.63
160	0.63	0.62	0.56	0.52	0.50	0.54	0.81	1.45	1.53	1.23	1.33	1.21	0.89	0.37
170	0.53	0.49	0.43	0.36	0.33	0.30	0.75	1.59	1.57	1.47	1.51	1.38	1.06	-
180	0.43	0.41	-	-	-	-	-	1.83	1.89	-	-	-	-	-

TABLE 5. Mass attenuation coefficient (μ/ρ) of Pt, Al and Ti in the 40 keV-100 keV energy range[21]

Energy (keV)	Pt	Al	Ti
40	12.45	0.57	2.21
50	6.95	0.37	1.21
60	4.34	0.28	0.77
80	8.73	0.20	0.41
100	4.99	0.17	0.27

Figure 5A anisotropy function for the non-shielded source is presented, in Figure 5B anisotropy function for the shielded source at Pt shield side and in Figure 5C anisotropy function for the shielded source at Al window side of the source is presented. In Figure 6 anisotropy function for three modes is presented. There are four graphs for distances of the evaluation point of the anisotropy function from the source: (A) 0.5 cm, (B) 2 cm, (C) 5 cm and (D) 12 cm distance.

Isodose curves (%) for the non-shielded source and the shielded source (Pt shield side) are plotted in Figure 7. In these plots the dose distributions were normalized to the dose at 1 cm distance from the source at transverse plane.

Discussion

In this study TG-43 dosimetric parameters for a 153Gd source with Pt shield were calculated for use in I-RSBT of prostate brachytherapy. Air kerma strength value for the non-shielded 153Gd source was found to be 6.71 U per 1 GBq activity.

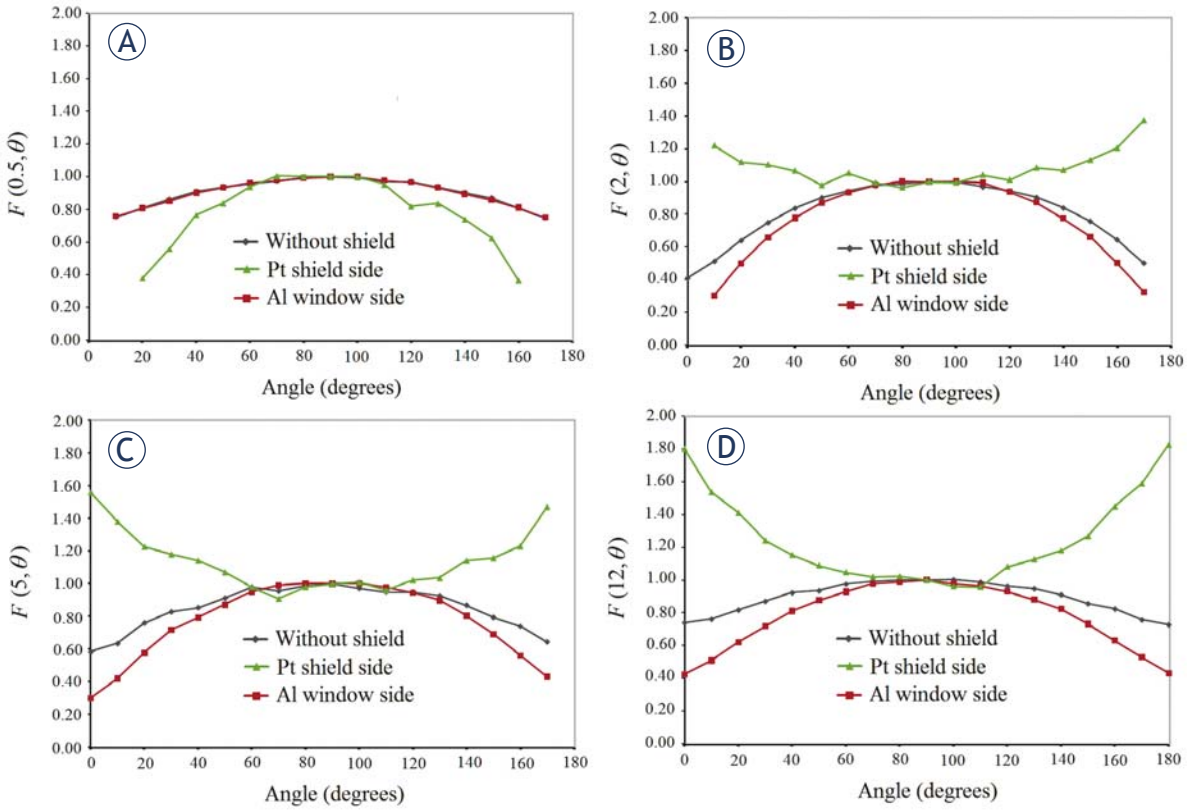

FIGURE 6. Comparison of anisotropy function for non-shielded mode, Pt shielded mode, Al window mode. All modes are presented for distances: **(A)** 0.5 cm, **(B)** 2 cm, **(C)** 5 cm, **(D)** 12 cm.

This means that 6.71 U of ^{153}Gd is equal to 27 mCi activity and 1U is equal to 4.03 mC activity. The results obtained in this study reveal that the ^{153}Gd dose rate constant is higher compared to the dose rate constant of ^{125}I source. This is due to the fact that average photon energy of ^{153}Gd is higher than that of ^{125}I (53.70 keV versus 28.37 keV). We found also that the simulated dose rate constant for non-shielded source is higher compared to the dose rate constant of shielded source. The reason for a higher dose rate constant in this case is the lower level of beam attenuation in non-shielded source compared to the shielded one. Furthermore I-RSBT source is two-part shielded (Pt shield and Al window Figure 1) where radiation attenuation at the Pt shield is higher compared to Al window. This effect can be explained by the values of the mass energy attenuation coefficients for Pt and Al, which are listed in Table 5. In the 153Gd photon energy range (40 keV to 100 keV), mass attenuation coefficient of Al is lower than Pt. Additionally there are also attenuations of the photons in the catheter and needle materials (Nitinol alloy of Ni and Ti elements) in the beam's path (Figure 1). Finally the radiation beam attenuation on the Al window side of the source is lower compared to the other Pt shield side of the source which is the essence of the I-RSBT.

In Figure 3A it can be seen that the trend of radial dose function is falling with distance. According to this chart, at distances less than 1 cm, the red graph which corresponds to existence of Al window is higher than the blue graph (related to the source without shield). Beyond the 1 cm distance the value of radial dose function for the non-shielded mode is higher compared to Al window case. It is due to lower attenuation of photons in Al window material. The calculated treatment dose should normally include a factor accounting for the attenuation of the material. In a treatment situation the rotating source with Al gap is "directed" to the tumor side which means that effective emission dwell times are longer in that situation. Consequently the dose received by the tumor is relatively higher compared to the healthy tissue. As it can be seen in Figure 3B, radial dose function is increasing with radial distance, and this is due to the density of platinum. The distance could be plotted

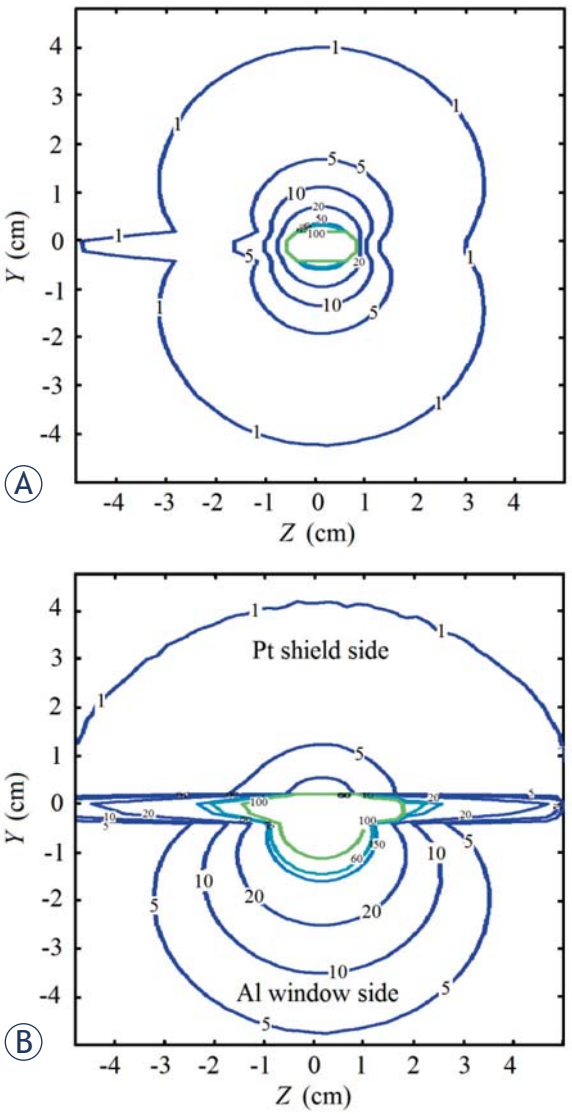

FIGURE 7. Isodose curves (%): **(A)** non shielded source, **(B)** shielded source. The dose distributions were normalized to the dose at 1 cm distance from the source at transverse plane. The *Z* axis is on the longitudinal axis of the source.

in terms of *r*×Pt density and the data be normalized to the dose rate at 1 cm physical distance from source center for the density corrected value. That way the trend of radial dose function may not be increasing.

In the calculation of radial dose function in Figure 3, each case was normalized to the dose value at 1 cm of itself. Based on Figure 3A the radial dose function in the Al window side is lower. This is due to higher photon attenuation in Al than in the water. Figure 3B, which corresponds to the Pt shield side, the radial dose function at the Pt shield side has increasing trend up to the distance of about 8 cm. In Figure 4 all the obtained dose values in three cases (non-shielded, Pt shield, Al window) were normalized to dose at 1 cm distance of the non-shield mode. With this calculation, there is evidence to have more accurate comparison. The graph in Figure 4 reveals the dependence of the source distance to the point of absorbed dose in the phantom. By increasing that distance the dose becomes lower for all three cases. Secondly, the dose in the case of Pt shield side is lower than at the Al window side. Additionally the dose at the Al widow source is lower than at the non-shielded source. These two effects are related to different absorption coefficients in Pt, Al and phantom. Pt has higher absorption coefficient than Al and Al has higher absorption coefficient than phantom (*i.e* water).

Figure 5A is related to the non-shielded source. Figure 5B is related to the Pt window source. In case of Pt window that side of the source receive lower dose. It indicates that Pt side should be turned to the side of organs at risk which means that central areas of the organs will receive lower dose. According to Figure 5A and C it can be mentioned that anisotropy at Al window mode is lower than at the non-shielded mode of the I-RSBT source. This is due to the attenuation of radiation in Al. This effect is similar for the comparison of anisotropy of Pt shield side versus non-shielded case. In directions other than 90º, beam traverses through longer path inside the needle and source, therefore the beam attenuation is more pronounced. The higher beam attenuation results to lower doses at these angles. Calculating the anisotropy function we normalized it to the dose at 90º. Thus the lower isotropy at these angles can be explained. The lower isotropy in I-RSBT source is like a disadvantage, because it causes non-uniformity of tumor dose. The peripheral parts of the tumor receive systematically lower doses than the central ones. In the Figure 6, anisotropy function is further analyzed. We compared different shielding effects of the I-RSBT source at four different distances in the phantom. We compared the source without shield, Pt shielded source and the source with Al window. They were compared at each of the four distances (0.5 cm, 2 cm, 5 cm, and 12 cm). As it can be concluded from the charts, at 0.5 cm from the source the anisotropy functions for the non-shielded mode and Al Window mode are relatively the same. This is because of the similar magnitude of self-absorption in both modes. Increasing the distance from the source there is a change of energy spectrum of photons in the phantom. The differences become greater by increasing the distance

from the source. The reason for anisotropy function equality at a distance of 0.5 cm for these two modes is their almost equal self-absorption.

In Figure 7, isodose curves are plotted for both non-shielded and shielded cases. As it can be seen in the shielded source considerable dose reductions occur at the Pt shield side. Thus the organs at risk located near the shield side of the source receive significantly lower dose. Organs that are located at 1 cm distance from the source (Pt shield side) receive 5% dose. This relative dose value is reduced further to 1% when the distance is approaching 4 cm. It should be noted that the shield should be turned to the side of organs at risk, such as the rectum and bladder. In prostate cancer the total organ volume is tumor which is covered with many irradiation source dwell positions. Thus the optimization of treatment plan can compensate eventual cold spots from the individual source dwell positions. As it was mentioned in the study of Adams *et al.*[19], by adjusting the number of needles and dwell positions as well as the number of rotations per dwell position, prostate dose can be controlled. It seems that in I-RSBT treatment of prostate cancer of Adams *et al.*[19] the radiation sensitive organs at risk are protected receiving the relative lower dose compared to tumor dose. As a consequence some parts of the tumor can receive lower dose which has to be compensated extending the affected irradiation dwell times in the treatment plan calculations. Overall radiation time is thus prolonged using this irradiation technique. The I-RSBT could be promising also for some other sites in brachytherapy like gynecology or breast brachytherapy. It is interesting as a subject of further research.

Additionally, the dose distribution around the source in shielded mode is less symmetrical compared to unshielded source which could be accounted as a disadvantage (Figure 7). However this can be compensated in treatment planning. This leads to "Intensity Modulated Brachytherapy" which is considered as an innovation at this time. Only the future will show us the real possibilities of these new techniques. As it was aforementioned in the text, Adams *et al*.[19] have introduced the interstitial rotating shield brachytherapy using a ^{153}Gd source for brachytherapy of prostate. In the study they used Computed Tomography imaging to offer clinical data for the shielded source positioning and rotation in the treatment planning process. They used 19 needles and 16 rotational angles per dwell position of the ^{153}Gd source rotating shield for annonimized prostate patient. The dose-volume histograms from conventional brachytherapy with ^{192}Ir source were compared with those from I-RSBT with ^{153}Gd source. Our study continues the scientific efforts adding TG-43 simulated dose parameters which enable Treatment Planning Systems to calculate the I-RSBT doses in phantoms and tissues.

Conclusions

The calculated TG-43 dosimetric parameters in this study for a combination of the ^{153}Gd source and the shielded needle could be used in treatment planning system. Dose rate constant and radial dose function with the shielded sources are considerably different than the non-shielded sources. Further studies will be required to justify our Monte Carlo simulation parameters as dose calculation tools on a real human RANDO phantom. From clinical point of view there are some issues relating the tumor dose uniformity which is related to dose volume histograms. The I-RSBT source has lower dose isotropy which can lead to lack of uniformity distribution in the tumor. This can be compensated with new Treatment Planning Systems based on the live Monte Carlo calculations. These are topics for the future research. In our opinion I-RSBT technique has realistic chances in the "Intensity Modulated" development of future Brachytherapy.

Acknowledgement

The authors would like to thank Sabzevar University of Medical Sciences for financial support of this work.

References

1. *SEER stat fact sheets: Prostate cancer*. [citated 2016 Jun 21]. Available at: http://seer.cancer.gov/statfacts/html/prost.html
2. Theodorescu D, Mellon P, Krupski TL. *Prostate cancer: brachytherapy (radioactive seed implantation therapy).* [citated 2016 Jun 21]. Available at: www.emedicine.commed/topic3147.htm#section~pictures.
3. Meigooni A, Bharucha Z, Yoe-Sein M, Sowards K. Dosimetric characteristics of the bests double-wall ^{103}Pd brachytherapy source. *Med Phys* 2001; **28:** 2568-75. doi: 10.1118/1.1414007
4. Meigooni A, Zhang H, Clark J, Rachabatthula V, Koona R. Dosimetric characteristics of the new RadioCoil™ Pd103 wire line source for use in permanent brachytherapy implants. *Med Phys* 2004; **31:** 3095-105. doi: 10.1118/1.1809851
5. Bernard S, Vynckier S. Dosimetric study of a new polymer encapsulated palladium-103 seed. *Phys Med Biol* 2005; **50:** 1493-504. doi: 10.1088/0031-9155/50/7/012
6. Patel NS, Chiu-Tsao ST, Williamson JF, Fan P, Duckworth T, Shasha D, *et al*. Thermoluminescentdosimetry of the Symmetra™ ^{125}I model I25. S06 interstitial brachytherapy seed. *Med Phys* 2001; **28:** 1761-9. doi: 10.1118/1.1388218

7. Enger SA, Lundqvist H, D'AmoursM, Beaulieu L. Exploring ^{57}Co as a new isotope for brachytherapy applications. *Med Phys* 2012; **39:** 2342-5. doi: 10.1118/1.3700171

8. Bahreyni Toossi MT, Abdollahi M, Ghorbani M. A Monte Carlo study on dose distribution validation of GZP6 ^{60}Co stepping source. *Rep Pract Oncol Radiother* 2012; **18:** 112-6. doi: 10.1016/j.rpor.2012.10.004

9. Oliveira SM, Teixeira NJ, Fernandes L, Teles P, Vaz P. Dosimetric effect of tissue heterogeneity for ^{125}I prostate implants. *Rep Pract Oncol Radiother* 2014; **19:** 392-8. doi: 10.1016/j.rpor.2014.03.004

10. Rivard MJ, Coursey BM, DeWerd LA, Hanson WF, Huq MS, Ibbott GS, et al. Update of AAPM task group No.43 report: a revised AAPM protocol for brachytherapy dose calculations. *Med Phys* 2004; **31:** 633-74. doi: 10.1118/1.1646040

11. Slate LJ, Elson HR, Lamba MA, Kassing WM, Soldano M, Barrett WL. A Monte Carlo brachytherapy study for dose distribution prediction in an inhomogeneous medium. *Med Dosim* 2004; **29:** 271-8. doi: 10.1016/j.meddos.2004.02.002

12. Ghorbani M, Mehrpouyan M, Davenport D, Ahmadi Moghaddas T. Effect of photon energy spectrum on dosimetric parameters of brachytherapy sources. *Radiol Oncol* 2016; **50:** 238-46. doi: 10.1515/raon-2016-0019

13. Bahreyni Toossi MT, Ghorbani M, Akbari F, Mehrpouyan M, Sobhkhiz Sabet L. Evaluation of the effect of tooth and dental restoration material on electron dose distribution and production of photon contamination in electron beam radiotherapy. *Australas Phys Eng Sci Med* 2015; **39:** 113-22. doi: 10.1007/s13246-015-0404-z

14. Bahreyni Toossi MT, Ghorbani M, Akbari F, Sobhkhiz Sabet L, Mehrpouyan M. Monte Carlo simulation of electron modes of a Siemens Primus linac (8, 12 and 14 MeV). *J Radiother Prac* 2013; **12:** 352-9. doi: https://doi.org/10.1017/S1460396912000593

15. Weaver K. Anisotropy functions for I-125 and Pd-103 sources. *Med Phys* 1998; **25:** 2271-8. doi: 10.1118/1.598458

16. Rodríguez EA, Alcón EP, Rodriguez ML, Gutt F, de Almeida E. Dosimetric parameters estimation using PENELOPE Monte-Carlo simulation code: model 6711 a ^{125}I brachytherapy seed. *Appl Radiat Isot* 2005; **63:** 41-8. doi: 10.1016/j.apradiso.2005.02.004

17. EngerSA, Fisher DR, Flynn RT. Gadolinium-153 as a brachytherapy isotope. *Phys Med Biol* 2013; **58:** 957-64. doi: 10.1088/0031-9155/58/4/957

18. Du SS, Wu Z, Li WR, Zeng ZC, Chen G, Wang J. Comparison of three conformal radiotherapies in three dimensional dosimetric planning for prostate cancer and the effect on quality of life. *Chinese J Clin Rehabi* 2005; **9:** 27-9. doi: 10.3321/j.issn:1673-8225.2005.10.019

19. Adams QE, Xu J, Breitbach EK, Li X, Enger SA, Rockey WR, et al. Interstitial rotating shield brachytherapy for prostate cancer. *Med Phys* 2014; **41:** 051703. doi: 10.1118/1.4870441

20. Ghorbani M, Behmadi M. Evaluation of hypothetical ^{153}Gd source for use in brachytherapy. *Rep Pract Oncol Radiother* 2016; **21:** 17-24. doi: 10.1016/j.rpor.2015.05.005

21. *LBNL Isotopes Project-LUNDS Universitet*. [citated 2016 Jun 21]. Available at: http://nucleardata.nuclear.lu.se/toi/nuclide.asp?iZA=640153

22. Perez-Calatayud J, Ballester F, Das RK, DeWerd LA, Ibbott GS, Meigooni AS, et al. Dose calculation for photon-emitting brachytherapy sources with average energy higher than 50 keV: report of the AAPM and ESTRO. *Med Phys* 2012; **39:** 2904-29. doi: 10.1118/1.3703892

23. *NIST standard reference simulation website*. [citated 2016 Jun 21]. Available at: http://physics.nist.gov/PhysRefData/XrayMassCoef/ComTab/water.html

24. *NIST standard reference simulation website*. [citated 2016 Jun 21]. Available at: http://physics.nist.gov/PhysRefData/XrayMassCoef/tab3.html